

2023-12-15

Leaf thermal regulation strategies of canopy species across four vegetation types along a temperature and precipitation gradient

Zhou, Y

<https://pearl.plymouth.ac.uk/handle/10026.1/21659>

10.1016/j.agrformet.2023.109766

Agricultural and Forest Meteorology

Elsevier BV

All content in PEARL is protected by copyright law. Author manuscripts are made available in accordance with publisher policies. Please cite only the published version using the details provided on the item record or document. In the absence of an open licence (e.g. Creative Commons), permissions for further reuse of content should be sought from the publisher or author.

1 **Leaf thermal regulation strategies of canopy species across four vegetation types**
2 **along a temperature and precipitation gradient**

3

4 Yingying Zhou^{1,2}, Nawatbhris Kitudom^{1,2}, Sophie Fauset^{3*}, Martijn Slot⁵, Zexin
5 Fan^{1,4}, Jianping Wang⁶, Weiwei Liu⁷, Hua Lin^{1,4*}

6

7 ¹CAS Key Laboratory of Tropical Forest Ecology, Xishuangbanna Tropical Botanical
8 Garden, Chinese Academy of Sciences, Mengla, Yunnan 666303, China.

9 ²University of Chinese Academy of Sciences, Beijing 100049, China.

10 ³School of Geography, Earth and Environmental Sciences, University of Plymouth,
11 Plymouth, PL4 8AA, UK.

12 ⁴Ailaoshan Station for Subtropical Forest Ecosystem Studies, Xishuangbanna
13 Tropical Botanical Garden, Chinese Academy of Sciences, Jingdong, Yunnan 676209,
14 China.

15 ⁵Smithsonian Tropical Research Institute, Panama City 0843-03092, Panama

16 ⁶School of Information Engineering and Automation, Kunming University of Science
17 and Technology, Kunming 650000, China

18 ⁷Lijiang Forest Biodiversity National Observation and Research Station, Kunming
19 Institute of Botany, Chinese Academy of Sciences, Lijiang, Yunnan 674100, China.

20

21

22

23

24

25

26

27

28

29

30

31

32 **Abstract**

33 The ecophysiological processes of leaves are more related to leaf temperature
34 (T_l) than air temperature (T_a). Transpiration and leaf physical traits enable plants to
35 maintain T_l within a thermal range. However, it is challenging to quantitatively study
36 leaf thermal regulation strategies, due to the complex interaction between thermal
37 effects of transpiration and leaf physical traits. We utilized a 3-T method that
38 compares T_l, T_a, and T_n (the temperature of non-transpiring leaves) investigate
39 thermal regulation strategies of dominant canopy species in four vegetation types,
40 including a savanna woodland, a tropical rain forest, a subtropical evergreen broad-
41 leaved forest, and a temperate mixed forest. Our results indicate that the difference
42 between T_l and T_a decreased as the site mean temperature increased. Transpirational
43 cooling was strongest in savanna woodland, and decreased from the hottest site to the
44 coldest site. Without transpiration, sun-exposed leaves were consistently hotter under
45 sunshine than air. This physical warming effect increased from the hottest site to the
46 coldest site. We observed leaf area, water content and leaf angle played a significant
47 role in physical thermal regulation. The present research quantitatively measured leaf
48 thermal regulation strategies across a temperature and precipitation gradient, which
49 advances our understanding of how plants adapt to their thermal environments.

50

51 **KEYWORDS:** leaf temperature, leaf traits, physical thermal effect, transpirational
52 cooling, thermal regulation, thermal response

53

54 **INTRODUCTION**

55 Leaf temperature (T_l) is the direct micro-environment governing plant
56 ecophysiological processes (Gates, 1968; Slot and Winter, 2017), and further
57 determines ecosystem energy, water and carbon budgets (Rey-Sánchez et al., 2017;
58 Sánchez et al., 2009). However, leaf temperatures often deviate from air temperature
59 (T_a). Previous investigation across 62 species have revealed that in a 5°C environment,
60 leaf temperatures can be elevated by up to 10°C compared to the surrounding air
61 temperature. Conversely, in a 55°C environment, leaf temperatures can be
62 approximately 7°C lower than the ambient air temperature (Michaletz et al., 2015).
63 The temperature difference between leaf and air has also been observed to reached
64 18.3 °C in the Atlantic forest, Brazil (Fauset et al., 2018). Similar temperature
65 deviations from air temperature are also common in inanimate materials such as water
66 or metal due to their distinct physical properties, for example heat capacity,
67 reflectivity, and size. However, these properties of inanimate materials remain
68 constant regardless of the environment. In contrast, plant traits can adapt or acclimate
69 to various environments, enable them to maintain their leaf temperatures within a
70 specific range. Although the time required for traits to change may vary widely,
71 ranging from a few seconds (e.g. stomatal conductance and transpiration) to hundreds
72 of years, plant traits are flexible. The combination of all the physical traits (e.g.,
73 morphological traits, optical traits, material properties) and physiological leaf traits
74 (e.g., transpiration) that contribute to maintaining leaf temperatures within the optimal
75 temperature range for photosynthesis is referred as "thermal regulation" (Jones and

76 Rotenberg, 2011; Monteiro et al., 2016). It includes cooling effects in hot habitats and
77 warming effects in cool habitats. Thermal regulation, thermal tolerance, and thermal
78 avoidance together constitute thermal adaptation strategies of plants.

79 Thermal regulation capacities of leaves differ among species, and vary with the
80 environment (Fauset *et al.*, 2018). According to the regression slope of T_l vs. T_a (β),
81 three types of leaf thermal response have been identified: limited homeothermy ($\beta <$
82 1), poikilothermy ($\beta = 1$), and megathermy ($\beta > 1$) (Blonder and Michaletz, 2018).
83 Homeothermic leaves maintain T_l below T_a when T_a exceeds a certain threshold,
84 while poikilothermic leaves closely track T_a ($T_l = T_a$), and megathermic leaves
85 exhibit a faster increase in temperature compared to T_a . Generally, stronger thermal
86 regulation, including both warming and cooling is found under extreme thermal
87 environments (John-Bejai et al., 2013; Körner, 2016; Smith, 1978; Vogel, 2005),
88 while weaker thermal regulation is found in more optimal thermal environments
89 (Drake et al., 2020). However, the mechanisms underlying leaf thermal regulation
90 strategies across different environmental gradients have not been fully explored.

91 Leaf temperature is determined by a combination of leaf physical and
92 physiological traits and environmental conditions (Campbell and Norman, 1998;
93 Monteith and Unsworth, 2013; Nobel, 2005). Leaf traits related to radiation loading
94 and heat exchange impact leaf temperature. For example, optical traits, leaf size and
95 orientation determine radiation loading (Jones and Rotenberg, 2011; Lambers et al.,
96 1998), while material properties such as water content and density affect heat capacity
97 (Jones, 2014; Lambers et al., 1998); leaf shape and area are related to heat

98 conductance (g_{Ha}) (Leigh et al., 2012; Muller et al., 2021); Stomatal conductance (g_s)
99 and water vapor transport conductance (g_{va}) influence transpirational cooling (Gates,
100 2003; Jones and Rotenberg, 2011; Monteith, 1973; Muir, 2019). However, it is
101 challenging to study thermal effects of leaf traits in the field due to the high variability
102 of leaf traits and their interactions (Blonder et al., 2020; Kitudom et al., 2022). For
103 example, small leaves with dark color also have thin boundary layers, which
104 facilitates heat exchange, meanwhile their dark colors also enables them to absorb
105 more radiation. In reality, it is the coordination of multiple leaf traits that improves
106 plant adaptation to the primary stress under its specific environment. Not all leaf traits
107 contribute directly to thermal regulation. Therefore, some previous studies used
108 artificial leaves to quantitatively evaluate thermal effects of leaf traits under controlled
109 environments (Daudet et al., 1998; Fetcher, 1981; Vogel, 2009). Lin et al. (2017)
110 employed a method to quantitatively distinguish thermal effects of transpiration and
111 leaf physical traits *in situ*. This technique, called “3-T method” requires three
112 temperatures: the temperature of a control leaf (T_l), the temperature of a non-
113 transpiring leaf (T_n), and air temperature (T_a). Although the combination of T_l , T_n
114 and T_a has often been used to evaluate water stress, transpiration and stomatal
115 conductance (Jones, 1999; Jones et al., 2018; Jones and Rotenberg, 2011; Qiu et al.,
116 2002), Lin et al. (2017) firstly used it to quantify thermal regulation in the field. By
117 employing this method, researchers can effectively monitor the thermal effects of
118 transpiration and the physical traits of leaves separately, thereby revealing leaf
119 thermal regulation strategies and their response to the natural environment *in situ*.

120 Upper-canopy species are fully exposed to air and solar radiation. Compared
121 with shaded plants, they are more influenced by radiative heating, turbulent exchange,
122 and longwave radiation loss at night (Miller et al., 2021). Transient “lulls” in wind can
123 cause leaf temperature to rise by > 5 °C in just a few seconds (Vogel, 2005). The
124 highly exposed and fluctuating environment makes canopy leaves more susceptible to
125 temperature extremes. Maximum temperatures of upper-canopy leaves have been
126 shown to exceed photosynthetic thermal optima in several tropical forests (Doughty
127 and Goulden, 2008; Mau et al., 2018; Miller et al., 2021; Pau et al., 2018). In such a
128 fluctuating environment, traits associated with temperature regulation should incur
129 greater selective advantage than in understory conditions. In addition, understory
130 species are distributed in buffered micro-environments due to shading which might be
131 very different from the canopy environment (Vinod et al., 2023). Therefore, canopy
132 species more strongly reflect the interaction between plants and the local environment
133 (Still et al., 2021).

134 In the present research, we used the 3-T method to study thermal regulation
135 strategies of upper canopy species in a savanna woodland, a tropical rain forest, a
136 subtropical evergreen broad-leaved forest and a temperate mixed forest. Thermal
137 regulation strategies depend on the temperature and water status of the habitat (Fauset
138 et al., 2018; Gates, 2003; Jones and Rotenberg, 2011). We hypothesize that the
139 savanna species mainly depend on leaf physical traits to cool leaves due to limited
140 transpirational cooling under dry conditions; tropical rain forest species can utilize
141 both transpirational cooling and leaf physical traits to avoid high leaf temperatures;

142 while subtropical forest species exhibit weaker thermal regulation due to limited
143 thermal stress; the species in the temperate forest primarily rely on physical warming
144 to cope with cold stress.

145 MATERIALS AND METHODS

146 Study sites and plant species

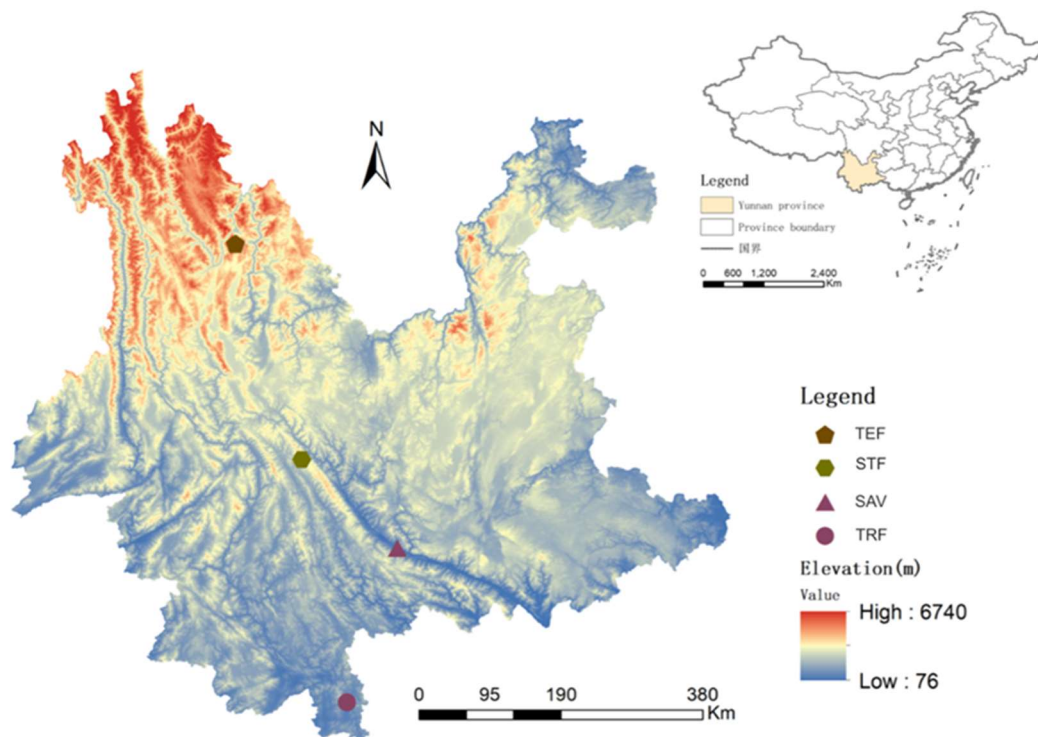


Figure 1 Site distribution.

147 We selected four vegetation types from the south to the north of Yunnan province,
148 China, including a savanna woodland (SAV), a tropical rain forest (TRF), a
149 subtropical broad-leaved forest (STF), and a temperate mixed forest (TEF) (Table 1
150 and Fig. 1). Four dominant upper canopy species were chosen in each site. These
151 species covered all the emergent species in TRF, all the canopy species in TEF, the
152 most abundant three species and the sixth most abundant canopy species in STF, and
153 the most abundant three species and the seventh most abundant species that grow

154 closely and under similar micro-habitat in SAV. Considering data balance across sites,
155 the replicate individuals were determined by the species with the smallest number of
156 individuals, thus three individuals were selected for each species. Detailed
157 information of the species can be found in Table S1.

158 **Measurement of thermal regulation strategies**

159 The 3-T method was used to measure thermal regulation strategies. This method
160 needs three temperatures: leaf temperature (T_l), leaf temperature of non-transpiring
161 leaf (T_n), and air temperature (T_a). The thermal effect of transpiration was calculated
162 by $T_l - T_n$ (Gates, 1968), and thermal effect of leaf physical traits compared with air
163 was calculated by $T_n - T_a$. Note that transpirational cooling refers to $T_n - T_l$, which
164 is therefore positive when there is a cooling effect. All the temperatures were
165 measured by T-type thermal couples (TT-T-30-SLE-1000, OMEGA, USA; diameter
166 = 0.25mm). To guarantee the accuracy of temperature measurements, we compared
167 leaf temperature difference (dT) between thermal couple and PT-100 (YAGEO
168 Nexensos GmbH, Germany) in the field. PT-100 is a platinum resistance temperature
169 detector (RTD) that utilizes the electrical resistance of platinum to measure
170 temperature. The accuracy of PT-100 is reported drift of 0 °C is 0.04% (0.16 °C) after
171 1000 hours at 400 °C in the field. The results showed thermocouple temperature
172 measurements are slightly higher, with an average dT of 0.6%. The maximum dT
173 reached 2.7% which happened after noon (Notes S3). Temperatures were recorded by
174 data logger (UX-120-04, HOBO, USA) every one minute from May 13 to May 16 at
175 TRF, May 19 to May 23 at STF, May 25 to May 28 at SAV, June 4 to June 7 at TEF

176 in 2019. This period was the most severe heatwave in Yunnan province from 1961 to
177 2019 (Kitudom *et al.*, 2022). At TRF and STF, crowns were accessed using canopy
178 crane infrastructure, whereas at the lower canopy sites SAV and TEF, they were
179 accessed from the ground or using a ladder. We used heat-conducting glue to fix the
180 thermal couple head on the adaxial side of the leaves. With this method, thermal
181 couples can be tightly fixed on leaves without impacting on stomata conductance and
182 avoid irradiation effects on the sensor head (Kitudom *et al.*, 2022). We put Vaseline
183 on the abaxial side of leaves to get non-transpiring leaves (all the leaves are
184 hypostomatous) (Gates, 1968; Jones, 1999). A thin layer of Vaseline on the abaxial
185 side of the leaf had negligible impacts on leaf physical thermal effects ((Thorpe and
186 Butler, 1977); Notes S1 and S2 for experimental tests and sensitivity analysis of the
187 impact of the Vaseline application). Temperatures of four mature, sun-exposed and
188 healthy control leaves, and two non-transpiring leaves of similar traits to the control
189 leaves were measured. Air temperatures beside these leaves were measured
190 simultaneously with thermal couples on the abaxial sides of leaves to avoid direct
191 solar radiation. Ten-minute average temperatures were used for analysis. T_n might be
192 lower than T_l due to water adhering to the Vaseline surface. This situation often
193 happened at night and in the early morning. However, $T_n < T_l$ also occasionally
194 happened during daytime in TEF, which might be because of weak transpirational
195 cooling. Therefore, a small change of leaf angle, wind and radiation loading of the
196 non-transpiring and the control leaf could induce negative $T_n - T_l$. We assumed
197 transpirational cooling was zero ($T_n = T_l$) when $T_n < T_l$.

198 **Leaf traits measurement**

199 We selected leaf traits that might be related to leaf temperature including
200 morphological, optical, anatomical, physiological traits and material properties (Table
201 2). Leaves for morphological traits measurement were collected adjacent to the leaves
202 for temperature measurements for 8–10 leaves per individual and 3 individuals per
203 species. All the leaves were scanned on a flatbed-scan scanner. Leaf area (Area), leaf
204 perimeter (P), perimeter/area ratio (P/A), leaf length (Length), and leaf width (Width)
205 were analyzed by ImageJ 1.52q based on the scanned image. Leaf angle was
206 measured using the “Measure” app on Apple’s iPhone (Apple Inc.). The horizontal
207 position is set at 0 degrees, with the leaf facing downwards, the angle is negative, and
208 the angle is positive when the leaf is facing upwards. Ten leaves of each individual
209 were used to measure reflectivity (R), transmissivity (T), and absorptivity (A) at
210 wavelength between 400nm and 700nm with an integrated sphere connected to a
211 spectrometer (USB2000, Ocean Optics, USA), and greenness with a chlorophyll
212 meter (SPAD-502, Minolta, Japan). Leaf water content (WC) and leaf density was
213 measured by weighing 3–8 leaves (more leaves for low-weight leaves) for each
214 individual. WC was calculated by the ratio of weight difference between fresh and dry
215 leaves to the dry mass (Pérez-Harguindeguy et al., 2013). Leaf fresh mass density
216 (Density.f) and leaf dry mass density (Density.d) were calculated as the ratio of leaf
217 fresh and dry mass to leaf volume respectively (Pérez-Harguindeguy et al., 2013).
218 Leaf volumes were determined by the water displacement method. Four leaves of
219 each individual were used to measure anatomical traits. Leaf thickness (Thickness),

220 the thickness of upper and lower epidermis (Epidermis_up, Epidermis_low), palisade
221 mesophyll (Thickness_palisade) and spongy mesophyll (Thickness_spongy) were
222 measured using paraffin cross section. Paradermal sections were cut from the middle
223 part of the leaf avoiding major veins. Paradermal sections for stomata measurement
224 were boiled in water for 10–15 min, then immersed in a 1:1 mixture of 30% H₂O₂ and
225 glacial acetic acid aqueous solution until being soft and disintegrated, after which we
226 carefully separated the epidermis. Paradermal sections for vein analysis were
227 bleached with 5% NaOH until they became transparent. Paradermal sections for
228 stomata and vein analysis were stained in 1% safranin diluted with ethanol for 15 min
229 before taking photos under a light microscope. Stomatal density was calculated by the
230 number of stomata divided by the area of view. Vein density was calculated by the
231 total length of veins per area. Diurnal patterns in transpiration rate, photosynthesis
232 rate, and stomatal conductance were measured with a Portable Photosynthesis system
233 (LI-6400, LICOR, USA) using a transparent leaf chamber. Temperature, light,
234 relative humidity and CO₂ concentration during the measurements were maintained at
235 ambient conditions (Fig. S1) and not controlled. The flow rate was 500 μmol·s⁻¹. For
236 each individual, three leaves next to the leaves for temperature measurements, were
237 measured repeatedly from morning to afternoon depending on solar radiation and the
238 availability of the canopy crane at each site (SAV: 8:00–17:00; TRF: 9:20–14:40;
239 STF: 9:30–16:30; TEF: 8:30–17:40). Gas exchange measurements were conducted for
240 two days in SAV, STF and TEF, and one day in TRF due to the unavailability of the
241 canopy crane. The maximum transpiration rate (Tr_{max}), photosynthesis rate (A_{max}) and

242 stomatal conductance (g_{\max}) were extracted from the diurnal measurements of leaf gas
243 exchange. These physiological traits might change with environment of measurement,
244 while the trend among species should be stable. Photosynthetic thermal tolerance was
245 measured with a PlanTherm PT100 (PSI, Czech Republic) based on the response of
246 basal chlorophyll *a* fluorescence to temperature (F_o -T curve) with three sun leaves for
247 each individual (details can be found in Kitudom et al., 2022). Leaf segments (2cm×
248 1cm) were heated by water bath from 25 °C to 70 °C. Heating rate was 2 °C min⁻¹.
249 T_{crit} was calculated as the intersection of lines extrapolated from the slow and fast
250 rising portions of F_o -T curve (Knight and Ackerly, 2002).

251 **Meteorological measurements**

252 Meteorological data were obtained from the measurements on towers above the
253 canopy in SAV, TRF, and STF. Meteorological data of TEF were obtained from a
254 weather station installed in the open land at a distance of 10 meters from the forest.
255 Air temperature, relative humidity, wind speed, and downward solar radiation (DR)
256 were sampled at 0.5 Hz using CR1000 dataloggers (Campbell Scientific, Inc, USA) at
257 each site. Ten-minute averages were used in the present study. The details of
258 mounting heights and instruments are shown in table S2.

259 **Data analysis**

260 Individual tree averages of leaf temperature, leaf thermal effects and leaf traits were
261 used for analysis. Considering that transpirational cooling only happened during
262 daytime and the variance of nighttime physical thermal effects were small among
263 species in each site and nighttime cooling is more effected by environmental factors

264 and canopy characteristics rather than physiological processes of plants, the following
265 analysis only used daytime values ($DR > 100 \text{ w}\cdot\text{m}^{-2}$).

- 266 • Patterns of parameters across biomes

267 Differences in leaf temperature, thermal effects of leaf physical traits and
268 physiological traits, and leaf traits among sites were analyzed by multiple
269 comparisons of least significant difference (LSD) (Steel et al., 1997).

- 270 • Leaf thermal response type

271 We calculated β as the slope of the regression line between T_a and T_l for each species.

272 We then used the “slope. Test” function in R package “smart” to test the difference
273 between β and 1. A β value is significantly smaller than 1 ($P < 0.05$) indicates
274 limited homeothermy; β that is not significantly different from 1 ($P > 0.05$) indicates
275 poikilothermy; and if β is significantly larger than 1 ($P < 0.05$), this species exhibits
276 megathermy.

- 277 • The relationship between thermal adaptation strategies

278 We used Pearson correlation to analyze the relationships between leaf temperature
279 regulation strategies (transpirational cooling and physical warming during daytime)
280 and photosynthetic thermal tolerance.

- 281 • The impact of microclimate and leaf traits on thermal regulation strategies

282 To analyze the different impacts of climate on leaf temperature regulation, the
283 correlations between leaf temperature metrics (T_l , dT , physical warming effect, and
284 transpirational cooling) and climate parameters (T_a and DR) were calculated using
285 Spearman’s rank correlation. Here, dT is the temperature difference between leaf and

286 air. Correlation coefficients were expressed as $r.Tl_Ta$, $r.Tl_DR$, $r.dT_Ta$, $r.dT_DR$,
287 $r.physic_Ta$, $r.physic_DR$, $r.trans_Ta$ and $r.trans_DR$, which were put into a PCA.
288 This separated species out according to their relationships between leaf temperature
289 metrics with Ta and DR , and allowed us to analyze which of these relationships are
290 most important for this separation. This was performed using the “prcomp” function
291 in base R. We further assessed how the position of the species is related to the species’
292 traits. This was performed using “env_fit” in the “vegan” package.

293 To identify key traits related to transpirational cooling and physical warming
294 during daytime ($DR > 100 \text{ w}\cdot\text{m}^{-2}$), Bayesian mixed effects models were used. For the
295 model examining the relationship between the maximum transpiration rate and
296 transpirational cooling (trans), the fixed effect was the maximum transpiration rate
297 (Tr_{max}) and the random effects were site and species (Eq. 1).

$$298 \quad \text{trans} = Tr_{max} + 1|\text{Site} + 1|\text{Species} \quad (1)$$

299 In the model exploring the relationship between the physical traits and physical
300 warming (physic), many physical leaf traits could impact physical warming. To avoid
301 high correlated traits in the regression model, these traits were categorized into four
302 groups: morphological traits, optical traits, material properties, and anatomical traits.
303 Pearson correlation was used to identify which traits that had significant correlations
304 with leaf physical warming. The traits with the strongest or significant correlations
305 with physical warming in each group were selected. We further checked collinearity
306 among these traits using pairwise Pearson correlation. If the correlation coefficient
307 was higher than 0.7, one of the two traits was removed. The retained leaf traits (Angle,

308 P, Greenness, WC, Density.d, Vein density and Palisade) were set as fixed effects for
309 the full model (Eq. 2), with site and species serving as random effects. The fixed
310 effects were center scaled to a mean of 0 with standard deviation of 1. According to
311 the correlation between leaf angle and physical warming, the absolute values of leaf
312 angle had a higher correlation with physical warming, therefore we used the absolute
313 values of leaf angle.

$$314 \text{ physic} = |\text{Angle}| + \text{P} + \text{Greenness} + \text{WC} + \text{Density.d} + \text{Vein density} + \text{Palisade} + \\ 315 \quad 1|\text{Site} + 1|\text{Species} \quad (2)$$

316 We constructed linear mixed regression models in a Bayesian framework using R
317 package “brms” (Burkner, 2017). We fit models with student_t priors for all the
318 coefficients, because the sample size was small and the population variance was
319 unknown. Four Markov Chain Monte Carlo (MCMC) chains were used to sample
320 from the posterior distribution of the regression parameters for each model, with 3000
321 iterations per chain. Half of the iterations were used for warming up. Chains
322 convergence was diagnosed by Rhat values equal to 1. For the full model of the
323 association of leaf physical traits to physical warming, no coefficient was significant.
324 To identify the best model, we dropped traits from the full model one by one, and
325 used WAIC values for model selection. Conditional R^2 and Marginal R^2 were
326 calculated using the r^2 function in the “performance” R package (Lüdtke et al.,
327 2021). Effect size was calculated by the following equation (Le Provost et al., 2020):

$$328 \text{ Effect size} = \frac{\alpha_i}{\sum_1 \alpha} mR^2 \quad (3)$$

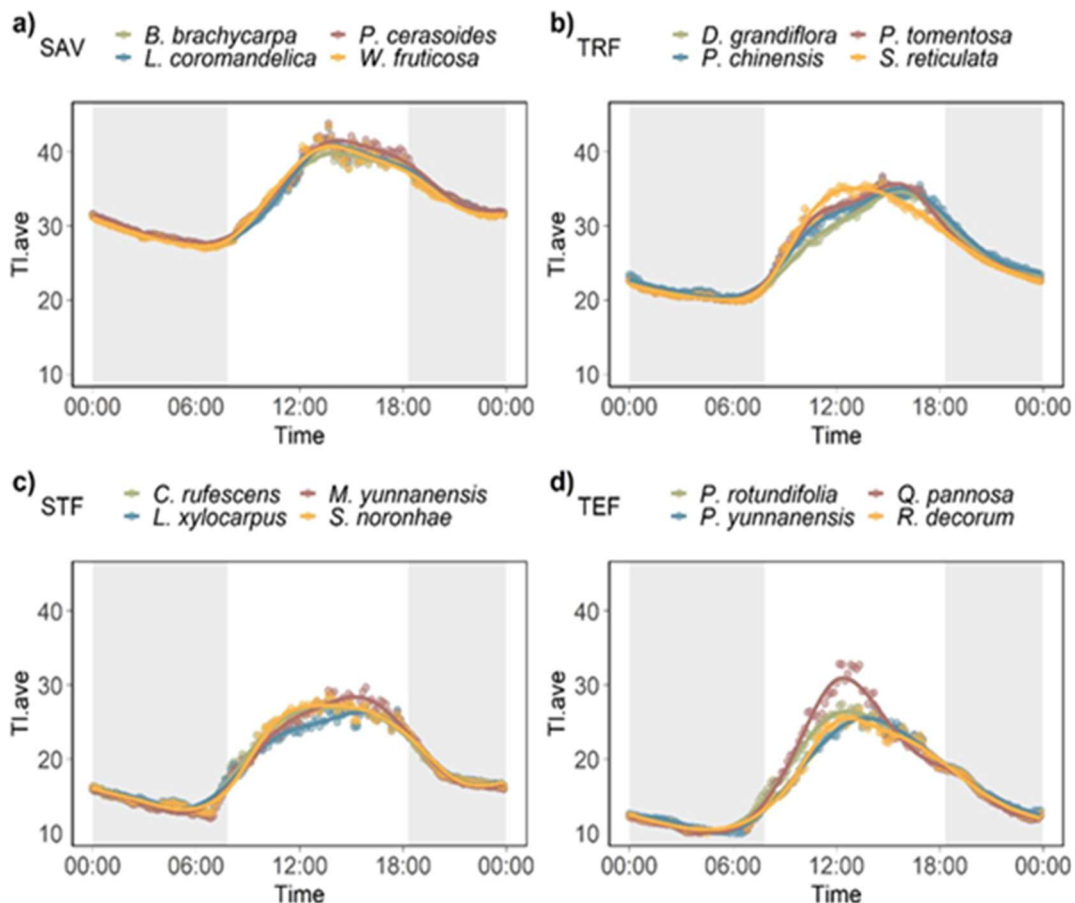
329 Where α_i is the coefficient of the fixed effect i , mR^2 is the marginal R^2 of the model. If
 330 the model had no random effects, mR^2 equals the R^2 of the model.

331 We found a non-linear relationship between leaf area and leaf physical
 332 warming. To investigate this relationship, we separately analyzed two ranges of leaf
 333 area ($< 50 \text{ cm}^2$ and $\geq 50 \text{ cm}^2$) using Pearson correlation. In addition, we employed
 334 Pearson correlation was used to examine the relationship between leaf traits and
 335 microclimate parameters with leaf physical warming at each site. Correlations were
 336 considered significant at $P < 0.05$.

337

338 RESULTS

339 Leaf temperature patterns across and within sites



340

Figure 2 Diurnal leaf temperatures (10 min average). Shading areas indicate nighttime. SAV, savanna woodland; TRF, tropical rain forest; STF, subtropical evergreen broad-leaved forest; TEF, temp mixed forest.

341 Leaf temperatures increased from TEF to SAV. The minimum leaf temperatures
 342 ranged from 8.4 ± 0.11 °C in TEF to 26.2 ± 0.11 °C in SAV. The maximum leaf
 343 temperatures ranged from 33.3 ± 2.07 °C in TEF to 46.0 ± 0.51 °C in SAV (Table 3).
 344 Daily leaf temperature ranges of TRF and TEF species were higher than STF and
 345 SAV species ($P = 0.003$). Of all the species, *Q. pannosa* in TEF had the highest daily
 346 leaf temperature range (25.9 ± 1.85 °C), and *B. brachycarpa* in SAV had the lowest
 347 daily leaf temperature range (16.4 ± 0.52 °C) (Fig. 2). The maximum leaf

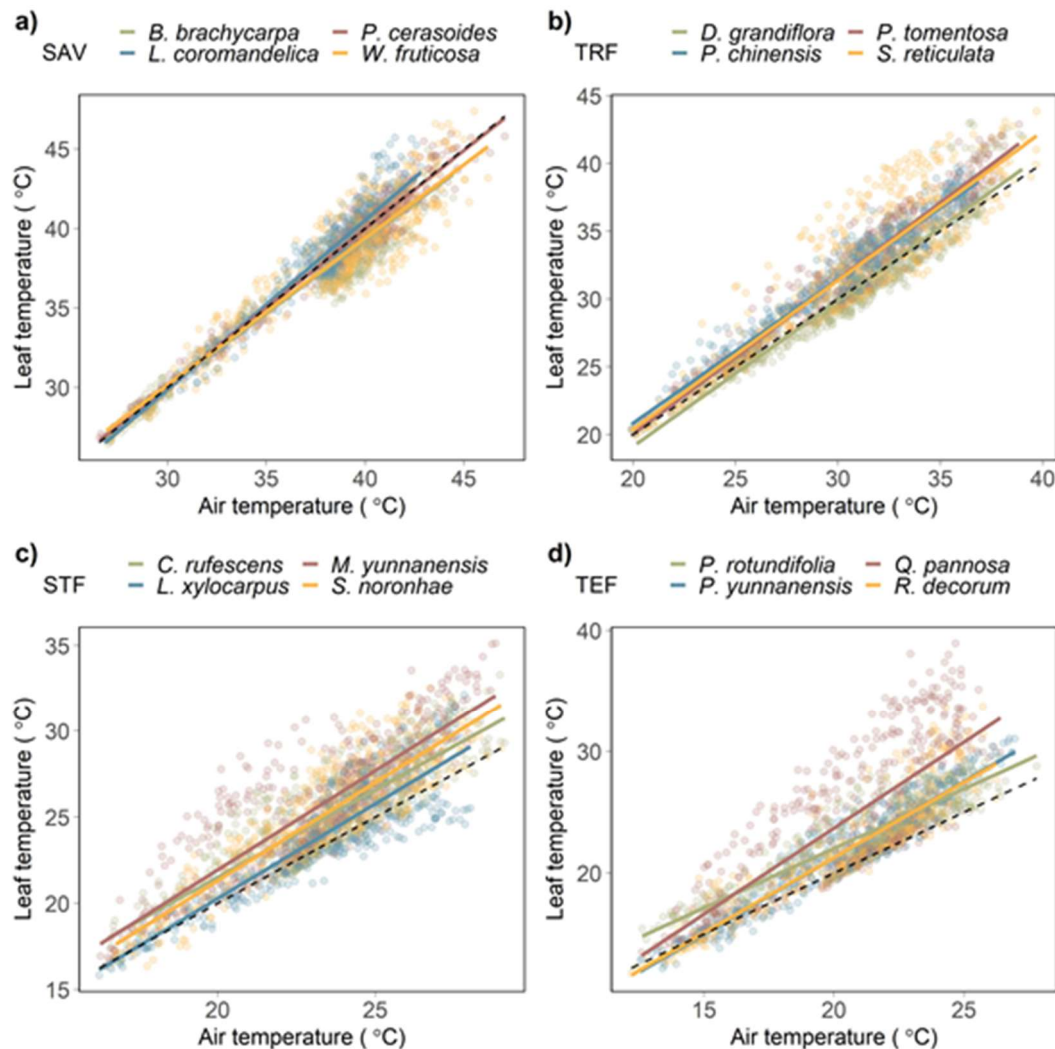


Figure 3 Linear regression between air temperature and leaf temperature. The slope of the dashed line is 1. SAV, savanna woodland; TRF, tropical rain forest; STF, subtropical evergreen broad-leaved forest; TEF, temperate mixed forest.

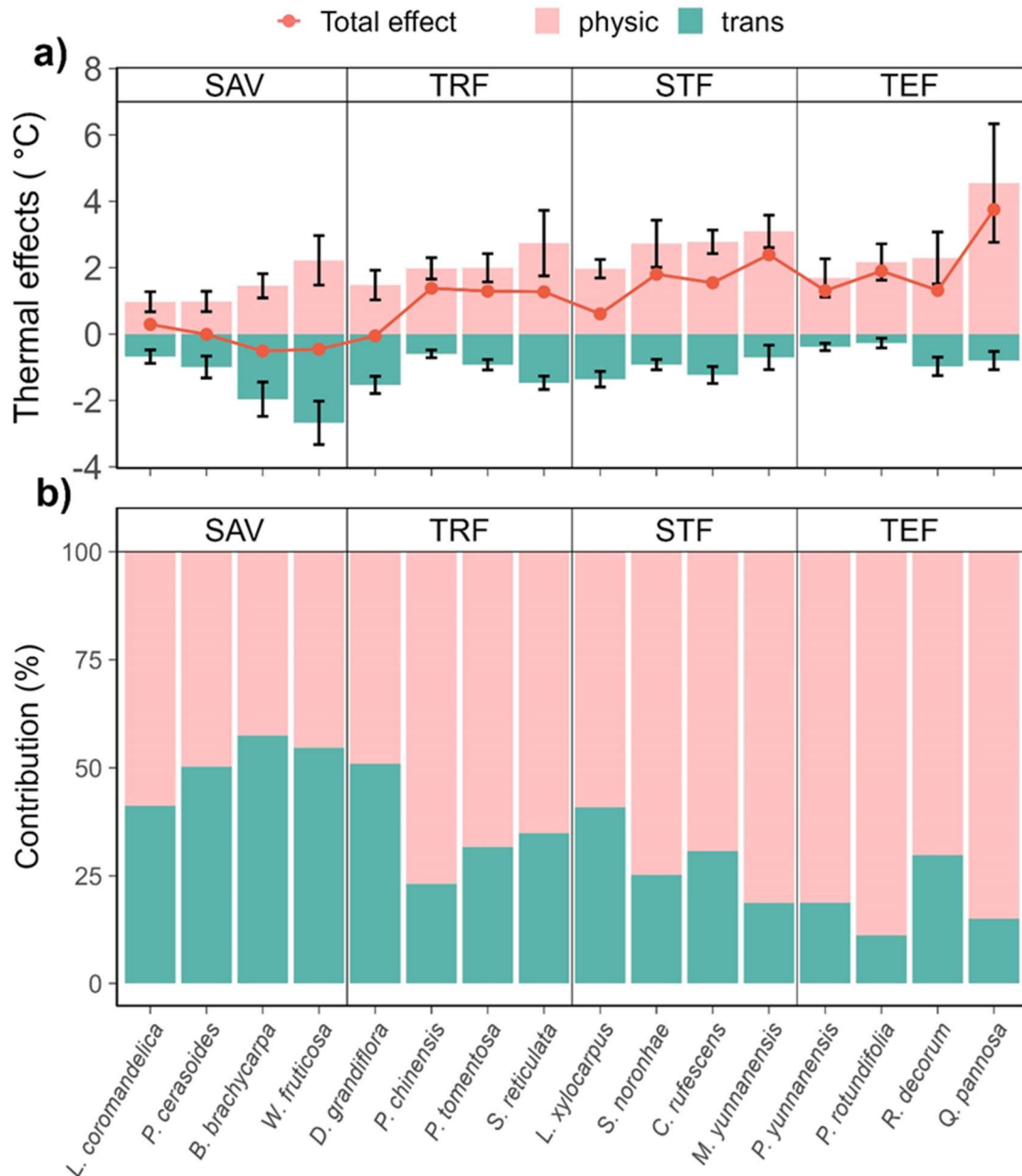
348 temperatures also varied among species within sites. Within each site, the maximum
349 leaf temperature variances among species were 1.2 °C, 1.8 °C, 2.9 °C and 13.6 °C in
350 SAV, TRF, STF, and TEF respectively.

351 Leaf temperatures of SAV species were closest to air temperature. Site mean
352 temperature difference between leaf and air (dT) decreased with site mean
353 temperature ($P < 0.001$) (Table 3). SAV species *P. cerasoides* and *W. fruticosa*
354 exhibited poikilothermic characteristics ($\beta = 1$); SAV species *B. brachycarpa* showed
355 limited homeothermy ($\beta < 1$); and all the other species displayed megathermy ($\beta > 1$)
356 (Fig. 3). Although β of TEF species *P. rotundifolia* was below 1, its leaf temperatures
357 were consistently higher than air temperature.

358 **Thermal regulation strategies across and within sites**

359 Compared with air temperature, physical traits had warming effects on leaves during
360 daytime and cooling effects during nighttime (Fig. S2). All the species showed the
361 strongest transpirational cooling before or around the time of peak air temperature,
362 except for *L. coromandelica* in SAV (Fig. S3). The physical daytime warming and
363 nighttime cooling effects were positively correlated across sites (Pearson correlation =
364 0.74, $P = 0.001$), however nighttime cooling was very weak and differences among
365 species were small. Thus, the following analysis only includes physical warming and
366 transpirational cooling during daytime ($DR > 100 \text{ w}\cdot\text{m}^{-2}$). Generally, the plants in the
367 hotter sites exhibited stronger transpirational cooling and less physical warming. For
368 three of the SAV species (*B. brachycarpa*, *W. fruticosa*, and *P. cerasoides*) and one
369 TRF species (*D. grandiflora*), the main thermal regulations were transpirational

370 cooling. Among them, *B. brachycarpa* and *W. fruitcosa* had the strongest
371 transpirational cooling of all the species (Fig. 4a). In contrast, the species in the cold
372 sites tended to have limited transpirational cooling, with *P. rotundifolia* and *P.*
373 *yunnanensis* in TEF forest showing the weakest transpirational cooling. Physical
374 warming dominated thermal regulation strategies for the species in TRF, STF and
375 TEF, except for *D. grandiflora* in TRF (Fig. 4a). The contribution of physical
376 warming to thermal regulation increased from the hot sites to the cold sites. TEF
377 species *Q. pannosa* had the strongest physical warming (Fig. 4b).



378

Figure 4 Leaf temperature regulation strategies. a). Thermal effects of transpiration and leaf physical traits during daytime; b). The contribution of transpirational cooling and leaf physical warming to the temperature difference between leaf and air. SAV, savanna woodland; TRF, tropical rain forest; STF, subtropical evergreen broad-leaved forest; TEF, temperate mixed forest.

379 **The impact of microclimate and leaf traits on thermal regulation strategies**

380 The correlation of leaf temperature metrics (TI, dT, transpirational cooling, and

381 physical warming) with Ta and DR separated species out. PC1 explained 39% and

382 PC2 explained 29% of the variance. PC1 was dominated by the positive relationship
383 between Tl and DR, and the negative relationships between transpirational cooling
384 and both Ta and DR. Species with high scores on this axis (*P. rotundifolia*, and *M.*
385 *yunnanensis*) had stronger positive relationships of Tl with DR, dT with Ta and DR,
386 and negative relationship of transpirational cooling with Ta and DR, hence displayed
387 less transpirational cooling and high leaf temperature under hot and bright conditions.
388 Species with low scores on this axis (*P. cerasoides*, *W. fruticosa*, and *B. brachycarpa*)
389 had stronger positive relationships of transpirational cooling with Ta and DR, and
390 therefore displayed stronger transpirational cooling under hot and bright conditions,
391 and accordingly, the leaf temperature did not increase strongly under increasing light
392 intensity. PC2 was dominated by the positive relationship between physical warming
393 and DR. The species with high scores on this axis (*P. tomentosa*, and *P. chinensis*) had
394 stronger positive relationships between physical warming and DR, therefore displayed
395 more physical warming under bright conditions. Species with low scores on this axis
396 (*P. rotundifolia*, and *L. xylocarpus*) showed weaker positive relationships between
397 physical warming and DR, therefore displayed less physical warming compared with
398 other co-existing species under bright conditions (Fig. 5).

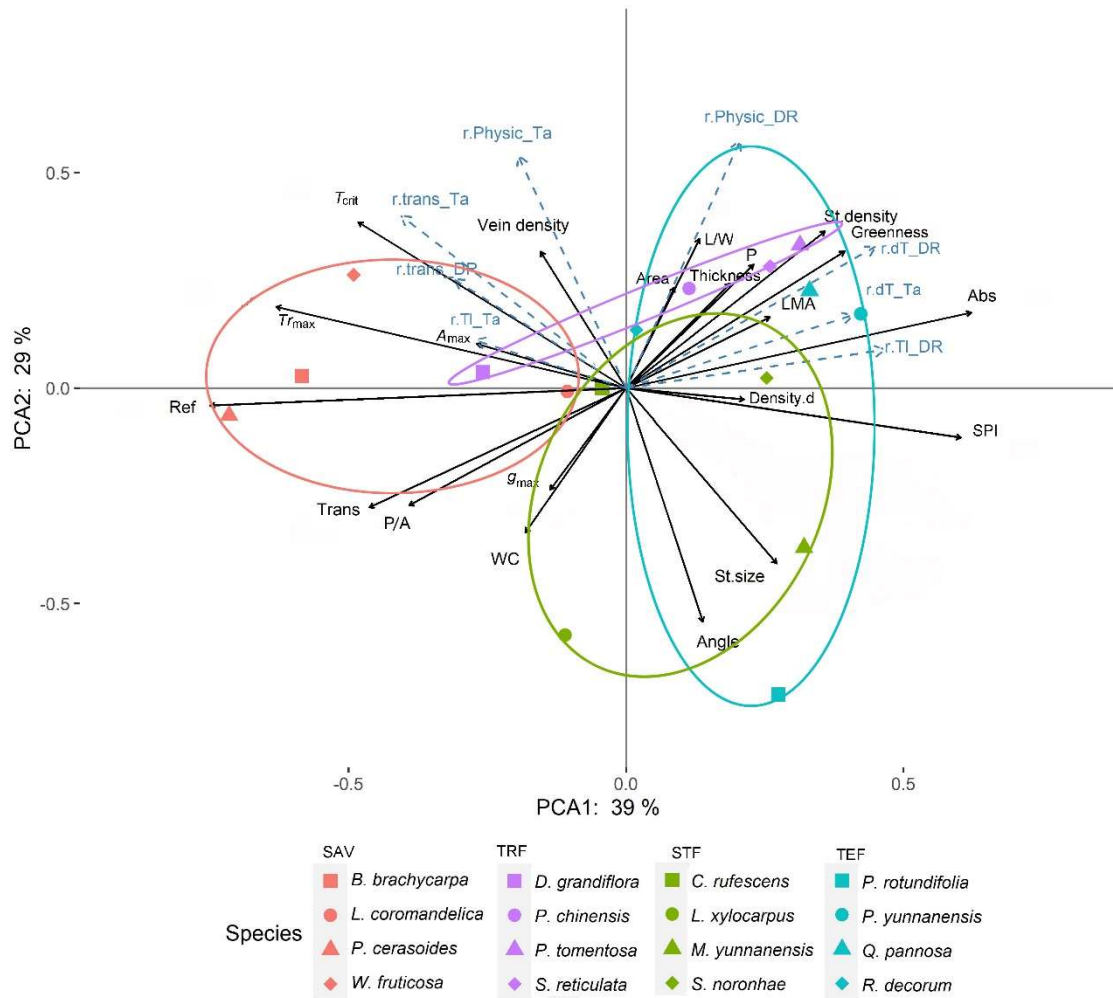


Figure 5 Principal component analysis of the relationship between thermal regulation strategies and climate factors and leaf traits. $r.trans_DR$, Pearson correlation coefficient between transpirational cooling and downward solar radiation (DR); $r.trans_Ta$, Pearson correlation coefficient between transpirational cooling and air temperature (Ta); $r.physic_DR$, Pearson correlation coefficient between physical warming and DR; $r.physic_Ta$, Pearson correlation coefficient between physical warming and Ta; $r.dT_Ta$, Pearson correlation coefficient between temperature difference between leaf and air (dT) and Ta; $r.dT_DR$, Pearson correlation coefficient between dT and DR; $r.Tl_DR$, Pearson correlation coefficient between leaf temperature (Tl) and DR; $r.Tl_Ta$, Pearson correlation coefficient between Tl and Ta. SAV, savanna woodland; TRF, tropical rain forest; STF, subtropical evergreen broad-leaved forest; TEF, temperate mixed forest.

400 With reference to plant traits, PC1 was dominated by gas exchange. Species with low
 401 values canceled out their heating with transpirational cooling (Fig. 4b), potentially
 402 giving them a photosynthetic advantage. These species also had high reflectance. PC2
 403 was positively related to leaf size (Area and L/W), greenness and stomatal density,
 404 while negatively related to WC and g_{\max} (Fig.5). Therefore, large leaves had stronger
 405 physical warming under bright conditions, however, this warming effect can be
 406 balanced by WC. The maximum stomatal conductance was coupled with leaf shape
 407 and water content (Fig. 5).

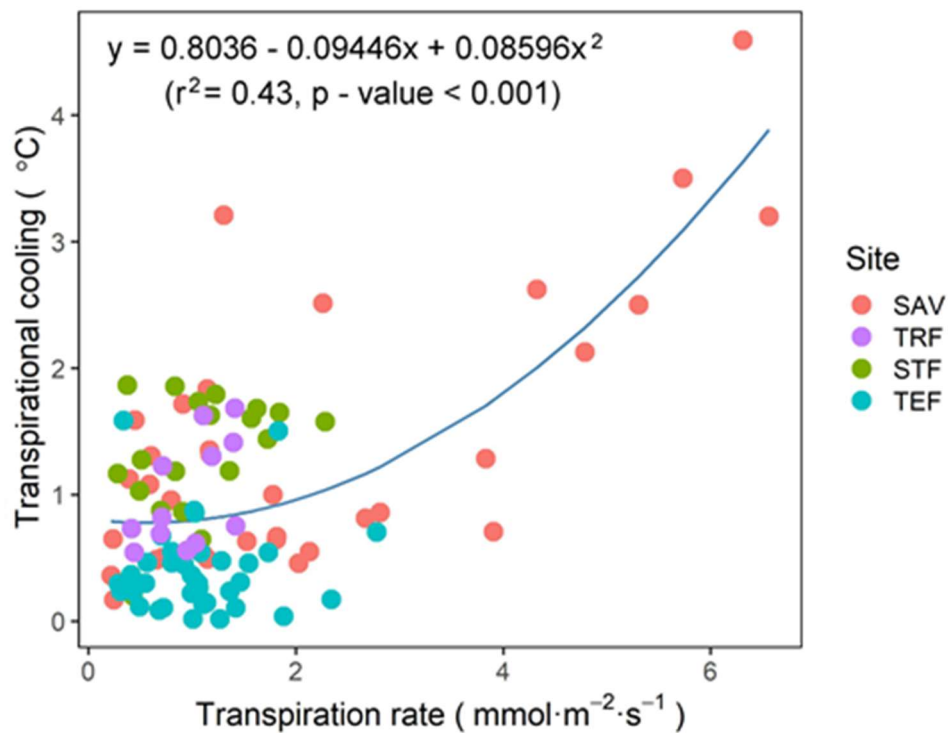


Figure 6 The relationship between transpirational cooling and transpiration rate. SAV, savanna woodland; TRF, tropical rain forest; STF, subtropical evergreen broad-leaved forest; TEF, temperate mixed forest.

408 Bayesian linear mixed regression showed that the marginal R^2 between the
 409 maximum transpiration rate and transpirational cooling was 0.461. Instantaneous

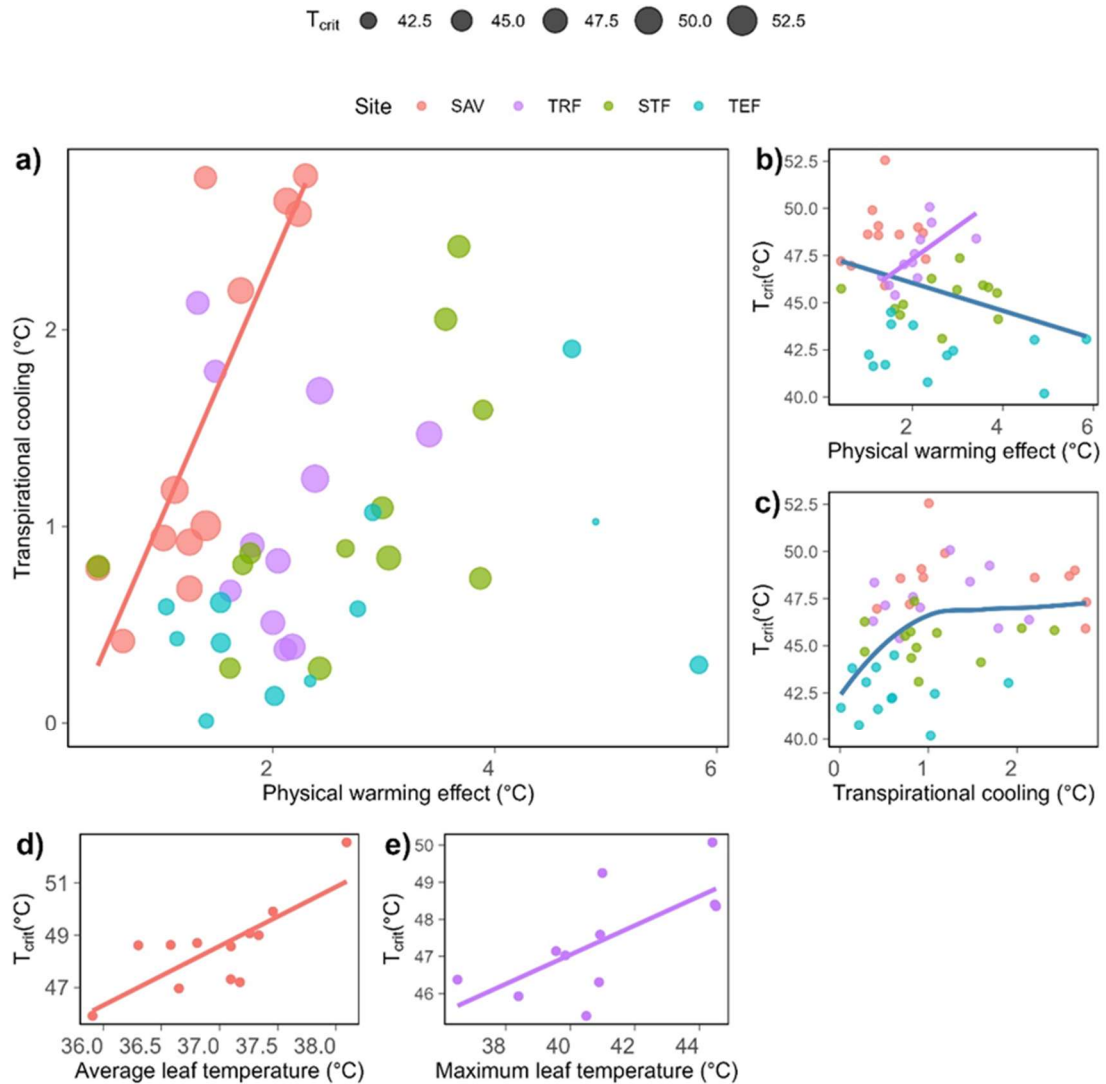
410 transpiration rates and transpirational cooling presented a quadratic relationship,
411 however, the relationship was weak when the transpiration rate was below 2.5
412 $\text{mmol}\cdot\text{s}^{-1}\cdot\text{m}^{-2}$ (Fig. 6). The best Bayesian mixed regression model showed that only
413 WC or Angle had significant negative relationships with physical warming effects,
414 with a marginal R^2 0.213 and R^2 0.114 respectively. There was a significant positive
415 correlation between leaf areas and physical warming effects for leaves smaller than 50
416 cm^2 (Pearson correlation = 0.52, $P = 0.005$), whereas the correlation turned negative
417 for leaves larger than 50 cm^2 (Pearson correlation = -0.74, $P = 0.03$).

418 The leaf traits and microclimate parameters that had high correlation with leaf
419 physical warming differed among sites. The significantly correlated leaf traits and
420 microclimate parameters were WC, optical traits (Trans, Ref, Abs and Chl),
421 physiological traits (Tr_{\max} , A_{\max} , and g_{\max}), Vein density and Ta_{\max} in SAV; WC, L/W,
422 leaf physiological traits (Tr_{\max} , A_{\max} , and g_{\max} , T_{crit}), Epidermis_up, and Ta_{\max} in TRF;
423 leaf material property (density.d and WC) and SPI in TEF. No significant correlations
424 between leaf traits and microclimate parameters and leaf physical warming were
425 found in STF (Fig. S4).

426 **The relationship between thermal adaptation strategies**

427 Transpirational cooling and physical warming effects showed positive correlation
428 across sites, but these correlations were significant only for SAV species within sites
429 (Pearson correlation = 0.96, $P = 0.04$) (Fig. 7a). Thermal tolerance was negatively
430 correlated with physical warming effects across sites (Pearson correlation = - 0.31, P
431 = 0.03), while a significant positive correlation was found for TRF species (Pearson

432 correlation = 0.67, $P = 0.02$) (Fig. 7b). Photosynthetic thermal tolerances increased
 433 with transpirational cooling, asymptoting when thermal tolerance reached 46 °C (Fig.
 434 7c). All four SAV species were deciduous, and shed leaves during dry season, which
 435 enables them to avoid heat stress when water is limited. Therefore, thermal regulation,
 436 thermal tolerance and thermal avoidance support thermal adaptation of SAV species
 437 together. In the two hot forests, thermal tolerance was positively correlated to leaf
 438 temperature (Pearson correlation = 0.77, $P = 0.003$ in SAV, and Pearson correlation =
 439 0.7, $P = 0.02$ in TRF) (Fig. 6d-e).



440

Figure 7 The relationship between thermal adaptation strategies. T_{crit} , photosynthetic thermal tolerance; SAV, savanna woodland; TRF, tropical rain forest; STF, subtropical evergreen broad-leaved forest; TEF, temperate mixed forest.

441 **DISCUSSION**

442 **Thermal regulation strategies across a temperature and precipitation gradient**

443 Transpirational cooling and physical warming effects of leaves varied with vegetation
444 types along a temperature and precipitation gradient. The first two hypotheses that
445 leaf physical cooling dominates leaf regulation strategies for the savanna species, and
446 that both transpirational cooling and leaf physical traits are important for leaf cooling
447 for the tropical rain forest species, were not fully supported by our results. Instead,
448 transpirational cooling prevailed in thermal regulation of SAV species, in addition to
449 leaf physical traits to reduce physical warming. TRF species presented moderate
450 transpirational cooling and physical warming. The hypotheses regarding thermal
451 regulation strategies of STF and TEF species were supported by our results.

452

453

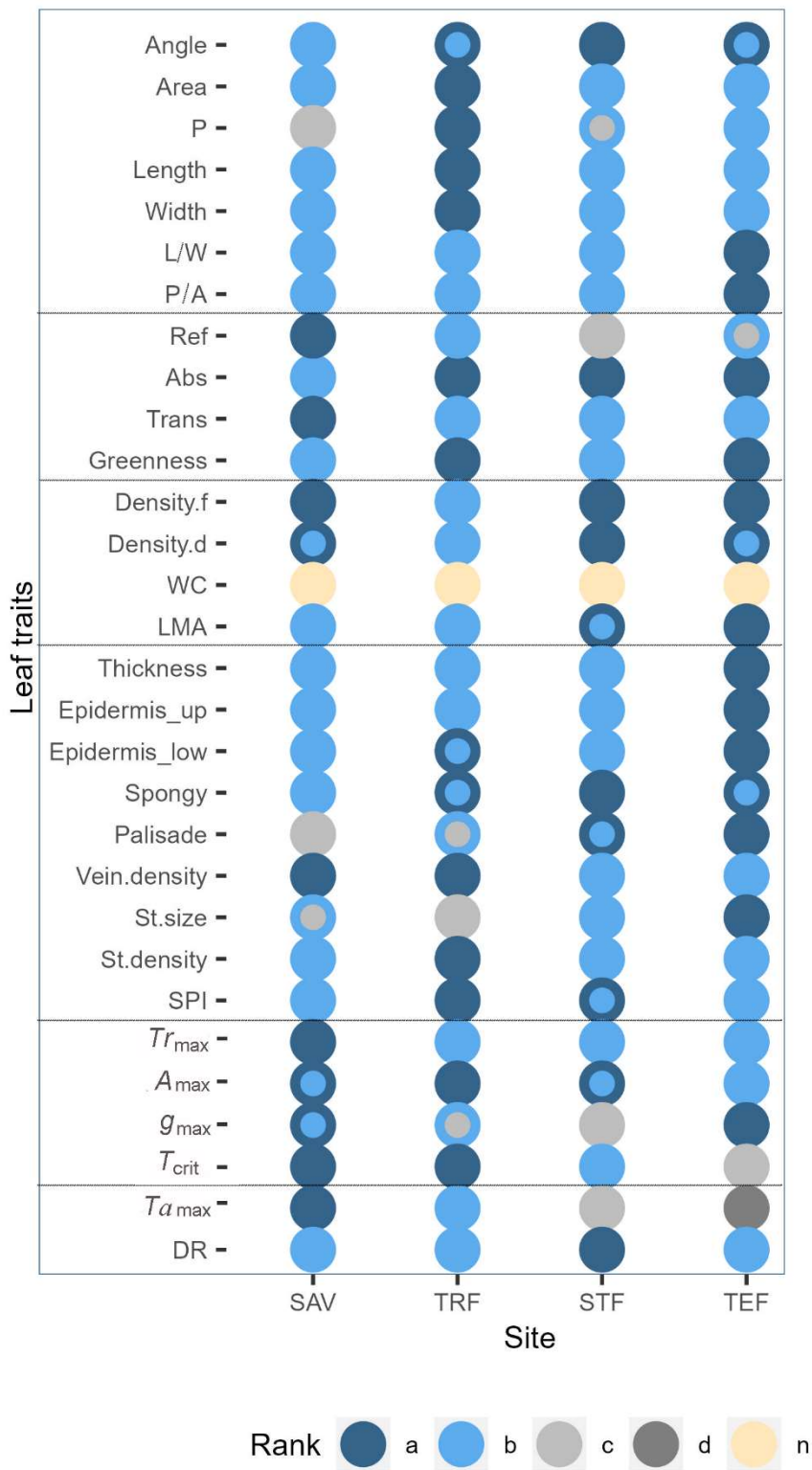


Figure 8 Multiple comparison of leaf traits and microclimate parameters among sites. SAV, savanna woodland; TRF, tropical rain forest; STF, subtropical evergreen broad-leaved forest; TEF, temperate mixed forest. Different color means significant difference. The same color means no significant difference. Values decreased from a to d.

455 The results showed that plants in the hot environment mainly relied on transpirational
456 cooling to avoid high leaf temperatures (Fig. 4). An increasing number of studies have
457 reported increased transpiration rates at high temperature (Crawford et al., 2012; Lin
458 et al., 2017; Sadok et al., 2021; Slot et al., 2016; Urban et al., 2017), even under
459 drought conditions (Aparecido et al., 2020; Smith, 1978; Urban et al., 2017).
460 Transpirational cooling may thus be even more important in arid and hot
461 environments due to its high cooling efficiency and its greater plasticity than leaf
462 physical traits. High VPD in a dry environment can facilitate transpirational cooling
463 as long as the stomata remain open. Although high thermal tolerance can partially
464 compensate for weak transpirational cooling, we did not find this pattern in our
465 research. On the contrary, both transpirational cooling and thermal tolerance increased
466 with environment temperature until thermal tolerance reached a saturation point (Fig.
467 7c). In addition, reducing physical warming is necessary for the plants in hot-dry
468 environment. SAV species had the lowest absorptivity and the highest reflectivity (Fig.
469 8), so that they can alleviate radiation loading, and hence showed low values of
470 physical warming (Fig. 4a). In addition to thermal regulation, species in the hot sites
471 (SAV and TRF) also had high photosynthetic thermal tolerance (Kitudom et al. 2022),
472 which would enable them to operate within their thermal safety margin. Most species
473 in SAV are deciduous species. On one hand, shedding leaves during the dry season
474 can further avoid heat damage (Zhang et al., 2012). On the other hand, deciduous
475 species usually had higher water and carbon exchange rate than evergreen species, so
476 that they can grow fast during the growing season and reduce leaf temperature with

477 high transpiration rates (Tomlinson et al., 2013). This demonstrates that plants can
478 utilize multiple methods to alleviate heat stress in extremely hot environments,
479 therefore there is no trade-off between thermal regulation, thermal tolerance and
480 thermal avoidance.

481 In cooler forests, the primary stress may shift from heat to other elements such
482 as coldness, light, or herbivory. Consequently, the strategies for adapting to heat
483 become weaker or shift towards cold adaptation. For instance, the offset of physical
484 warming through transpirational cooling diminishes (Fig 7a), and the relationships
485 between thermal tolerance and leaf temperatures vanish in cool forests (Fig 7d and e).
486 TEF species have developed mechanisms to increase leaf temperature to adapt to low
487 temperatures. Transpiration always cools leaves; generally, only leaf physical traits,
488 except for thermogenesis, can have warming effects. Accordingly, physical warming
489 dominated thermal regulation for the species in cold regions. Take *Q. pannosa* as an
490 example, it has the lowest water content and high absorptivity and density, as well as
491 being covered by dense brown trichome on the abaxial side of the leaf. As a result, *Q.*
492 *pannosa* showed the strongest physical warming among all the species. In addition to
493 leaf traits at the leaf level, some other traits at branch and canopy level also contribute
494 to leaf temperature regulation. For instance, the emergent trees in TRF promote
495 convection compared to a more even canopy; most of the TEF species have short
496 petioles and clustered leaves, which increases the thickness of the insulating boundary
497 layer (Michaletz and Johnson, 2006; Smith and Carter, 1988). For the species without
498 specific traits to resist the cold, shedding leaves during winter is a final solution. The

499 ambient temperature in STF is cool, with few extreme temperatures, therefore we did
500 not find any leaf physical trait significantly related to physical warming (Fig. S4).
501 Even so, the dense and even canopy at STF could provide a heat buffer to extreme
502 temperatures. In brief, plants under extreme thermal environment can utilize all means
503 to optimize performance and survive. Integrating studies at leaf, branch and canopy
504 levels can reveal the mechanisms for plant adaptations to the thermal environment.

505 **Leaf regulation strategies among species**

506 Even under the same environment, plants might adopt different leaf thermal
507 regulation strategies. Pioneer species typically show more active metabolism (Bazzaz,
508 1979), hence stronger transpirational cooling. In SAV, *W. fruticosa* and *B.*
509 *brachycarpa* are shrubs. They have much higher photosynthetic and transpiration
510 rates, shorter leaf life span (Zhang, 2007; Zhang et al., 2019) and high branch die
511 back ratio compared with the other two tree species (Chen et al., 2021). They showed
512 strong transpirational cooling. To balance transpirational cooling and water shortage,
513 *W. fruticosa* develops few small leaves; *B. brachycarpa* folds leaves under strong
514 solar radiation (Crawford et al., 2012; Lin et al., 2017). Blonder & Michaletz (2018)
515 and Blonder et al. (2023) proposed that stomatal optimization models should consider
516 additional optimization criteria related to avoiding thermal mortality under extreme
517 hot environment. Generally, photosynthesis and transpiration are coupled because
518 both CO₂ and water vapor enter and exit through the stomata. However, under
519 extreme high temperature, transpiration might increase regardless of photosynthesis
520 (Drake et al., 2018; Feng et al., 2023; Urban et al., 2017). *W. fruticosa* and *B.*

521 *brachycarpa* represented low water use efficiency when exposed to high temperatures
522 (Fig. S5), indicating that they may adjust their stomata to prioritize leaf cooling over
523 carbon gain. Plants from various functional groups can employ a wide range of water
524 use strategies (Aparecido et al., 2020; Bueno et al., 2019; Gong et al., 2023). The
525 other two SAV species adopt more conservative water use strategies. The TRF
526 species *D. grandiflora* presented similar thermal regulation strategies to SAV species,
527 which involve high levels of transpirational cooling. However, *D. grandiflora* showed
528 higher water use efficiency during the daytime (Fig S5), suggesting that it may adjust
529 its stomata to maximize carbon gain instead. This species is characterized by
530 unusually large and evergreen leaves which had a disadvantage in heat dissipation.
531 Nonetheless, the high transpiration rate accompanied by high photosynthesis rate and
532 large leaves, benefit the maximization of carbon gain, enabling *D. grandiflora* to
533 quickly reach the canopy as a pioneer tree (Mo et al., 2013). In addition, heat stress in
534 TRF was not as strong as it is in SAV, allowing growth to be prioritized over avoiding
535 heat stress. Although *D. grandiflora* had the largest leaf size and absorptivity, its
536 physical warming was weakest among TRF species. Self-shading, more vertical leaf
537 angles, and high water content might play important roles in reducing and buffering
538 leaf temperature.

539 **The relationship between thermal response and thermal regulation**

540 Energy balance theory predicts that limited homeothermy ($\beta < 1$) occurs when
541 stomatal conductance is high and convective resistance is low; poikilothermy ($\beta = 1$)
542 occurs when convective resistance is low; megathermy ($\beta > 1$) occurs when

543 microclimate or trait parameters co-vary in certain ways with T_a , e.g. when incident
544 radiation or relative humidity increase with T_a (Blonder and Michaletz, 2018).
545 However, the relationships between β and the parameters of leaf traits and
546 environment are too complex to be simulated by a simple model. We can evaluate β
547 from the perspective of thermal regulation. When transpirational cooling is stronger
548 than physical warming, plants present homeothermy; when transpiration cooling
549 equals physical warming, plants present poikilothermy; when transpirational cooling
550 is weaker than physical warming, plants present megathermy. In the present study,
551 most species were megathermic; only two poikilothermic (*P. cerasoides* and *W.*
552 *fruticosa*) and one limited homeothermic species (*B. brachycarpa*) were found in
553 SAV. Our results suggest that plants present limited homeothermy at the biome scale,
554 as cooling effects were stronger in hotter environments and warming effects were
555 stronger in colder environments. However, at the species level, megathermy is more
556 typical for sun leaves in field conditions, which is in accordance with the finding from
557 Blonder & Michaeletz' leaf energy balance model (Blonder & Michaeletz, 2018). A
558 growing number of studies reports megathermy of sun leaves under sunshine (Fauset
559 et al., 2018; Still et al., 2022). Air is almost transparent to solar radiation, while leaves
560 can absorb more radiation than air, therefore thermal effects of leaf physical traits
561 always have a warming effect under solar radiation, if there is convective resistance.
562 Only when leaves are small and under strong wind, convective resistance becomes
563 insignificant (Muller et al., 2021). However, this situation was not common under
564 field conditions in our study. Reducing solar radiation loading is indeed another

565 mechanism to alleviate physical warming. For example, the desert plant *Welwitschia*
566 *mirabilis* achieves relatively low leaf temperature by high reflectivity and casting
567 shadow above the ground (Schulze et al., 1980). Although high reflectivity and low
568 absorptivity can reduce radiation loading, these factors are unlikely to reduce β below
569 1 without transpiration.

570 The limited homeothermy of *B. brachycarpa* can be a result of its high stomatal
571 conductance and small leaves (low convective resistance), and its capacity to fold
572 leaves to avoid radiation loading. Although *W. fruticosa* also had high stomatal
573 conductance, its strong physical warming balanced the cooling effect of transpiration,
574 therefore it presented poikilothermy. *P. cerasoides* and *L. coromandelica* had low
575 absorptivity, relatively small leaves, and more vertical leaf angles which can reduce
576 physical warming. However, transpirational cooling of *P. cerasoides* was stronger
577 than *L. coromandelica*, thus *P. cerasoides* presented poikilothermy, while *L.*
578 *coromandelica* presented megathermy. In TEF, wind speed was the highest among the
579 four sites. *P. rotundifolia*, which had $\beta < 1$, has long petioles. They can swing with
580 wind and leaf angle becomes steeper under high temperature, thus convection and
581 reducing radiation loading might be the main causes of low β for *P. rotundifolia*.

582 **3-T method for studying thermal regulation**

583 The 3-T method provided an effective and convenient way to study thermal regulation
584 strategies. It can be used to continuously monitor transpirational cooling and physical
585 thermal effects in the field, and it enables us to disentangle the potentially interacting
586 effects of transpiration and leaf physical traits. This method is not restricted to

587 application at the leaf level; it can also be used at the stand or community level. The
588 development of technology for achieving non-transpiring leaves is ongoing. Coating
589 leaves with Vaseline is a traditional way (Lin et al., 2017; Thorpe and Butler, 1977;
590 Wallace and Clum, 1938; Zhang et al., 2020). The main artifact of Vaseline coating is
591 the changes of the boundary layer (see Notes S1), which means that the coating must
592 be applied thinly and evenly ($\leq 3 \text{ mg} \cdot \text{cm}^{-2}$). Developing new materials and using
593 high-precision modeling to calculate T_n can further improve the accuracy of the 3-T
594 model.

595 There are some notes for the 3-T method. First, the leaf with Vaseline must
596 have similar leaf physical traits to the control leaf to minimize the influence on leaf
597 physical thermal effects; Second, if there was condensation or rain on leaves, water
598 would be retained longer on the Vaseline surface than leaves. T_n might be lower than
599 T_l when control leaves were dry while the Vaseline coated leaves were wet; Third, the
600 high temperature of T_n might damage leaf, the damaged leaf should be replaced in
601 time.

602 **CONCLUSION**

603 The present research used 3-T method to study thermal regulation strategies of leaves
604 along a temperature and precipitation gradient. We found higher transpirational
605 cooling in hotter sites and stronger physical warming in cooler sites. The results
606 highlight the key role of transpirational cooling in hot sites, even in an arid region.
607 Although leaf physical traits can relieve heat damage, no physical traits at the leaf
608 level can reduce leaf temperature equal to or below air temperature under solar

609 radiation. Among leaf physical traits, water content, leaf area and leaf angle play
610 significant role in regulating leaf physical thermal effects. The present research
611 revealed a relatively comprehensive scenario of leaf regulation strategies under four
612 distinct environments, thereby enhance our understanding of how plants adapt to
613 thermal environments.

614

615 **Acknowledgement**

616 This research is supported by the National Natural Science Foundation of China
617 [grant number 32171504 and 31870386], ANSO Scholarship for Young Talents
618 Award, Chinese Academy of Sciences President's International Fellowship Initiative
619 [grant number 2016VBA036], Top young talents of Yunnan high-level talent training
620 and support program [grant number YNWR-QNBJ-2019-191], Natural Environment
621 Research Council [grant number NE/V008366/1], West Light Talent Program of the
622 Chinese Academy of Sciences [xbzg-zdsys-202218] and the support of the 14th Five-
623 Year Plan of Xishuangbanna Tropical Botanical Garden, Chinese Academy of
624 Sciences. Thanks for the field work support from National Forest Ecosystem Research
625 Station at Xishuangbanna, National Forest Ecosystem Research Station at Ailaoshan,
626 Yuanjiang Savanna Ecosystem Research Station, Xishuangbanna Tropical Botanical
627 Garden, Chinese Academy of Sciences, Lijiang Forest Biodiversity National
628 Observation and Research Station, Kunming Institute of Botany, Chinese Academy of
629 Sciences, and the central laboratory of Xishuangbanna Tropical Botanical Garden,

630 Chinese Academy of Sciences. Thank Canopy Science Research Platform II for
631 facility and data supporting.

632

633 **Reference**

634 Aparecido, L.M.T., Woo, S., Suazo, C., Hultine, K.R. and Blonder, B., 2020. High
635 water use in desert plants exposed to extreme heat. *Ecol Lett*, 23(8): 1189-
636 1200.

637 Bazzaz, F.A., 1979. The physiological ecology of plant succession. *Annual Review of*
638 *Ecological Systematics*, 10: 351-371.

639 Blonder, B.W. et al., 2023. Plant water use theory should incorporate hypotheses
640 about extreme environments, population ecology, and community ecology.
641 *New Phytol*, 238: 2271-2283.

642 Blonder, B.W., Escobar, S., Kapas, R.E. and Michaletz, S.T., 2020. Low predictability
643 of energy balance traits and leaf temperature metrics in desert, montane and
644 alpine plant communities. *Funct Ecol*, 34(9): 1882-1897.

645 Blonder, B.W. and Michaletz, S.T., 2018. A model for leaf temperature decoupling
646 from air temperature. *Agr Forest Meteorol*, 262: 354-360.

647 Bueno, A. et al., 2019. Effects of temperature on the cuticular transpiration barrier of
648 two desert plants with water-spender and water-saver strategies. *J Exp Bot*,
649 70(5): 1613-1625.

650 Burkner, P.C., 2017. brms: An R package for Bayesian multilevel models using stan. *J*
651 *Stat Softw*, 80(1): 1-28.

652 Campbell, G.S. and Norman, J.M., 1998. *Introduction to environmental biophysics*.
653 Springer, New York, xxi, 286 p. pp.

654 Chen, Y.J. et al., 2021. Hydraulic prediction of drought-induced plant dieback and
655 top-kill depends on leaf habit and growth form. *Ecol Lett*, 24(11): 2350-2363.

656 Crawford, A.J., McLachlan, D.H., Hetherington, A.M. and Franklin, K.A., 2012. High
657 temperature exposure increases plant cooling capacity. *Curr Biol*, 22(10):
658 R396-R397.

659 Daudet, F.A., Silvestre, J., Ferreira, M.I., Valancogne, C. and Pradelle, F., 1998. Leaf
660 boundary layer conductance in a vineyard in Portugal. *Agr Forest Meteorol*,
661 89(3-4): 255-267.

662 Doughty, C.E. and Goulden, M.L., 2008. Are tropical forests near a high temperature
663 threshold? *J Geophys Res-Biogeophys*, 113: G00B07.

664 Drake, J.E. et al., 2020. No evidence of homeostatic regulation of leaf temperature
665 in *Eucalyptus parramattensis* trees: integration of CO₂ flux and oxygen isotope
666 methodologies. *New Phytol*, 228(5): 1511-1523.

667 Drake, J.E. et al., 2018. Trees tolerate an extreme heatwave via sustained
668 transpirational cooling and increased leaf thermal tolerance. *Global Change*
669 *Biol*, 24(6): 2390-2402.

670 Fauset, S. et al., 2018. Differences in leaf thermoregulation and water use strategies
671 between three co-occurring Atlantic forest tree species. *Plant Cell Environ*,
672 41(7): 1618-1631.

673 Feng, X.L., Liu, R., Li, C.J., Zhang, H. and Slot, M., 2023. Contrasting responses of
674 two C4 desert shrubs to drought but consistent decoupling of photosynthesis
675 and stomatal conductance at high temperature. *Environ Exp Bot*, 209: 105295.

676 Fetcher, N., 1981. Leaf size and leaf temperature in tropical vines. *American*
677 *Naturalist*, 117(6): 1011-1014.

678 Gates, D.M., 1968. Transpiration and leaf temperature. *Ann Rev Plant Physio*, 19:
679 211-238.

680 Gates, D.M., 2003. *Biophysical ecology*. Dover Publications, Mineola, N.Y.

681 Gong, X.W., Leigh, A., Guo, J.J., Fang, L.D. and Hao, G.Y., 2023. Sand dune shrub
682 species prioritize hydraulic integrity over transpirational cooling during an
683 experimental heatwave. *Agr Forest Meteorol*, 336.

684 John-Bejai, C., Farrell, A.D., Cooper, F.M. and Oatham, M.P., 2013. Stress and
685 survival in tropical environments contrasting physiological responses to excess
686 heat and irradiance in two tropical savanna sedges. *Aob Plants*, 5: plt051.

687 Jones, H.G., 1999. Use of thermography for quantitative studies of spatial and
688 temporal variation of stomatal conductance over leaf surfaces. *Plant Cell*
689 *Environ*, 22(9): 1043-1055.

690 Jones, H.G., 2014. *Plants and microclimate - a quantitative approach to environmental*
691 *plant physiology*. Cambridge University Press, University Printing House, UK.

692 Jones, H.G., Hutchinson, P.A., May, T., Jamali, H. and Deery, D.M., 2018. A practical
693 method using a network of fixed infrared sensors for estimating crop canopy
694 conductance and evaporation rate. *Biosyst Eng*, 165: 59-69.

695 Jones, H.G. and Rotenberg, E., 2011. *Energy, radiation and temperature regulation in*
696 *plants*. eLS. John Wiley & Sons, Chichester.

697 Kitudom, N. et al., 2022. Thermal safety margins of plant leaves across biomes under
698 a heatwave. *Sci Total Environ*, 806: 150416.

699 Knight, C.A. and Ackerly, D.D., 2002. An ecological and evolutionary analysis of
700 photosynthetic thermotolerance using the temperature-dependent increase in
701 fluorescence. *Oecologia*, 130(4): 505-514.

702 Körner, C., 2016. Plant adaptation to cold climates. *F1000Res*, 5: 2769.

703 Lambers, H., Chapin, F.S., III and Pons, T., 1998. Leaf energy budgets: effects of
704 radiation and temperature, *Plant Physiological Ecology*. Springer New York,
705 pp. 210-229.

706 Le Provost, G. et al., 2020. Land-use history impacts functional diversity across
707 multiple trophic groups. *P Natl Acad Sci USA*, 117(3): 1573-1579.

708 Leigh, A. et al., 2012. Do thick leaves avoid thermal damage in critically low wind
709 speeds? *New Phytol*, 194(2): 477-487.

710 Lin, H., Chen, Y.J., Zhang, H.L., Fu, P.L. and Fan, Z.X., 2017. Stronger cooling
711 effects of transpiration and leaf physical traits of plants from a hot dry habitat
712 than from a hot wet habitat. *Funct Ecol*, 31(12): 2202-2211.

713 Lüdecke, D., Ben-Shachar, M.S., Patil, I., Waggoner, P. and Makowski, D., 2021.

714 performance: An R package for assessment, comparison and testing of
715 statistical models. *Journal of Open Source Software*, 16(60): 3139.

716 Mau, A.C., Reed, S.C., Wood, T.E. and Cavaleri, M.A., 2018. Temperate and tropical
717 forest canopies are already functioning beyond their thermal thresholds for
718 photosynthesis. *Forests*, 9(1): 47.

719 Michaletz, S.T. and Johnson, E.A., 2006. Foliage influences forced convection heat
720 transfer in conifer branches and buds. *New Phytol*, 170(1): 197-197.

721 Michaletz, S.T. et al., 2015. Plant thermoregulation: Energetics, trait-environment
722 interactions, and carbon economics. *Trends Ecol Evol*, 30(12): 714-724.

723 Miller, B.D., Carter, K.R., Reed, S.C., Wood, T.E. and Cavaleri, M.A., 2021. Only
724 sun-lit leaves of the uppermost canopy exceed both air temperature and
725 photosynthetic thermal optima in a wet tropical forest. *Agr Forest Meteorol*,
726 301: 108347.

727 Mo, X.X., Shi, L.L., Zhang, Y.J., Zhu, H. and Slik, J.W.F., 2013. Change in
728 phylogenetic community structure during succession of traditionally managed
729 tropical rainforest in southwest china. *Plos One*, 8(7): e71464.

730 Monteiro, M.V., Blanusa, T., Verhoef, A., Hadley, P. and Cameron, R.W.F., 2016.
731 Relative importance of transpiration rate and leaf morphological traits for the
732 regulation of leaf temperature. *Aust J Bot*, 64(1): 32-44.

733 Monteith, J.L., 1973. Principles of environmental physics. Contemporary biology.
734 American Elsevier Pub. Co., New York,, xiii, 241 pp.

735 Monteith, J.L. and Unsworth, M.H., 2013. Principles of environmental physics :
736 plants, animals, and the atmosphere. Elsevier Academic Press, Amsterdam ;
737 Boston.

738 Muir, C.D., 2019. tealeaves: an R package for modelling leaf temperature using
739 energy budgets. *Aob Plants*, 11(6): plz054.

740 Muller, J.D., Rotenberg, E., Tatarinov, F., Oz, I. and Yakir, D., 2021. Evidence for
741 efficient nonevaporative leaf-to-air heat dissipation in a pine forest under
742 drought conditions. *New Phytol*, 232(6): 2254-2266.

743 Nobel, P.S., 2005. Physicochemical and environmental plant physiology. Elsevier
744 Academic Press, Amsterdam, Boston.

745 Pau, S., Detto, M., Kim, Y. and Still, C.J., 2018. Tropical forest temperature
746 thresholds for gross primary productivity. *Ecosphere*, 9(7): e02311.

747 Pérez-Harguindeguy, N. et al., 2013. New handbook for standardised measurement of
748 plant functional traits worldwide. *Aust J Bot*, 61(3): 167-234.

749 Qiu, G.Y. et al., 2002. Comparison of the three-temperature model and conventional
750 models for estimating transpiration. *Jarq-Japan Agricultural Research*
751 *Quarterly*, 36(2): 73-82.

752 Rey-Sánchez, A.C., Slot, M., Posada, J.M. and Kitajima, K., 2017. Spatial and
753 seasonal variation in leaf temperature within the canopy of a tropical forest.
754 *Clim Res*, 71(1): 75-89.

755 Sadok, W., Lopez, J.R. and Smith, K.P., 2021. Transpiration increases under high-
756 temperature stress: Potential mechanisms, trade-offs and prospects for crop
757 resilience in a warming world. *Plant Cell Environ*, 44(7): 2102-2116.

758 Sánchez, J.M., Caselles, V., Niclos, R., Coll, C. and Kustas, W.P., 2009. Estimating
759 energy balance fluxes above a boreal forest from radiometric temperature
760 observations. *Agr Forest Meteorol*, 149(6-7): 1037-1049.

761 Schulze, E.D., Eller, B.M., Thomas, D.A., von Willert, D.J. and Brinckmann, E., 1980.
762 Leaf Temperatures and Energy-Balance of *Welwitschia-Mirabilis* in Its
763 Natural Habitat. *Oecologia*, 44(2): 258-262.

764 Slot, M., Garcia, M.N. and Winter, K., 2016. Temperature response of CO₂ exchange
765 in three tropical tree species. *Funct Plant Biol*, 43(5): 468-478.

766 Slot, M. and Winter, K., 2017. In situ temperature response of photosynthesis of 42
767 tree and liana species in the canopy of two Panamanian lowland tropical
768 forests with contrasting rainfall regimes. *New Phytol*, 214(3): 1103-1117.

769 Smith, W.K., 1978. Temperatures of desert plants: another perspective on the
770 adaptability of leaf size. *Science*, 201(4356): 614-616.

771 Smith, W.K. and Carter, G.A., 1988. Shoot Structural Effects on Needle Temperatures
772 and Photosynthesis in Conifers. *Am J Bot*, 75(4): 496-500.

773 Steel, R.G.D., Torrie, J.H. and Dickey, D.A., 1997. Principles and procedures of
774 statistics - a biometrical approach. *Biometrics*. McGraw-Hill, New York.

775 Still, C.J. et al., 2022. No evidence of canopy-scale leaf thermoregulation to cool
776 leaves below air temperature across a range of forest ecosystems. *Proc Natl
777 Acad Sci U S A*, 119(38): e2205682119.

778 Still, C.J. et al., 2021. Imaging canopy temperature: shedding (thermal) light on
779 ecosystem processes. *New Phytol*, 230(5): 1746-1753.

780 Thorpe, M.R. and Butler, D.R., 1977. Heat transfer coefficients for leaves on orchard
781 apple trees. *Boundary-Layer Meteorology*, 12: 61-73.

782 Tomlinson, K.W. et al., 2013. Leaf adaptations of evergreen and deciduous trees of
783 semi-arid and humid savannas on three continents. *Journal of Ecology*, 101(2):
784 430-440.

785 Urban, J., Ingwers, M.W., McGuire, M.A. and Teskey, R.O., 2017. Increase in leaf
786 temperature opens stomata and decouples net photosynthesis from stomatal
787 conductance in *Pinus taeda* and *Populus deltoides x nigra*. *J Exp Bot*, 68(7):
788 1757-1767.

789 Vinod, N. et al., 2023. Thermal sensitivity across forest vertical profiles: patterns,
790 mechanisms, and ecological implications. *New Phytol*, 237(1): 22-47.

791 Vogel, S., 2005. Living in a physical world V. Maintaining temperature. *J Biosciences*,
792 30(5): 581-590.

793 Vogel, S., 2009. Leaves in the lowest and highest winds: temperature, force and shape.
794 *New Phytol*, 183(1): 13-26.

795 Wallace, R.H. and Clum, H.H., 1938. Leaf temperatures. *Am J Bot*, 25(2): 83-97.

796 Zhang, J.L., 2007. Phenology, leaf structure and function, and seasonal variation in
797 photosynthesis of woody plants in a dry-hot valley of Yuanjiang, southwestern
798 China, Xishuangbanna Tropical Botanical Garden, Kunming, Yunnan.

799 Zhang, J.L., Poorter, L., Hao, G.Y. and Cao, K.F., 2012. Photosynthetic
800 thermotolerance of woody savanna species in China is correlated with leaf life
801 span. *Annals of Botany*, 110(5): 1027-1033.

802 Zhang, S.B., Wen, G.J. and Yang, D.X., 2019. Drought-induced mortality is related to
803 hydraulic vulnerability segmentation of tree species in a savanna ecosystem.
804 Forests, 10(8): 697.

805 Zhang, Y. et al., 2020. A proposed method for simultaneous measurement of cuticular
806 transpiration from different leaf surfaces in *Camellia sinensis*. Front Plant Sci,
807 11: 420.

808

809 Table 1 Site information (Kitudom et al., 2022)

Site	Abbreviation	Location	Elevation (m)	MAP (mm)	MAT (°C)	Ta_{max} (°C)	Ta_{min} (°C)	RH (%)	Canopy height (m)
Savanna woodland	SAV	23°28'N, 102°10'E	481	733	25.0	45.1	26.5	62 (53)	4-6
Tropical rain forest	TRF	21°22'N, 101°34'E	704	1415	22.7	38.6	18.6	80 (65)	>50
Subtropical broad-leaved forest	STF	24°32'N, 101°02'E	2501	1931	11.8	28.7	12.2	81 (60)	25-30
Temperate mixed forest	TEF	27°00'N, 100°13'E	3240	1300	8.7	26.8	9.1	65 (57)	25-30

810

811 Ta_{max} and Ta_{min} , the maximum and minimum air temperature above the canopy during measurement, averaged by all the measure points on the
 812 canopy; MAP, mean annual precipitation; MAT, mean annual temperature; RH, average relative humidity in 2019, the values in brackets are the
 813 average RH during measurement.

814

815

816 Table 2 The investigated leaf traits (Kitudom et al., 2022).

Class	Leaf traits	Abbreviation (unit)
Morphological trait	Leaf Area	Area (cm ²)
	Perimeter	P (cm)
	Leaf length	Length (cm)
	Leaf width	Width (cm)
	Length/Width	L/W
	The ratio of perimeter to area	P/A (cm ⁻¹)
	Angle	Angle (°)
Optical trait	Reflectivity	Ref (%)
	Absorptivity	Abs (%)
	Transmissivity	Trans (%)
	Greenness	Greenness
Material property	Leaf fresh mass density	Density.f (g cm ⁻³)
	Leaf dry mass density	Density.d (g cm ⁻³)
	Water content	WC (%)
	Leaf mass per area	LMA (g cm ⁻²)
Anatomical trait	Leaf thickness	Thickness (μm)
	Thickness of upper epidermis	Epidermis_up (μm)
	Thickness of lower epidermis	Epidermis_low (μm)
	Thickness of spongy tissue	Spongy (μm)
	Thickness of palisade tissue	Palisade (μm)
	Leaf vein density	Vein density (mm ⁻¹)
	Stomata size	St.size (μm)
	Stomata density	St.density (No mm ⁻²)
	Stomata size ² × Stomata density	SPI (mm ⁻¹)
	Physiological trait	Maximum photosynthesis rate
Maximum transpiration rate		Tr_{\max} (mmol m ⁻² s ⁻¹)
Maximum stomatal conductance		g_{\max} (mol m ⁻² s ⁻¹)
Photosynthetic thermal tolerance		T_{crit} (°C)

817

818

819 Table 3 Range of leaf temperature (Tl) and temperature difference between leaf and
 820 air (dT).

Site	Tl range (°C)	dT range (°C)
	Mean ± SE	Mean ± SE
SAV	26.2 ± 0.11 ~ 46.0 ± 0.51	-1.3 ± 0.27 ~ 1.1 ± 0.43
TRF	18.2 ± 0.05 ~ 42.4 ± 0.91	-0.9 ± 0.11 ~ 2.5 ± 0.52
STF	11.1 ± 0.20 ~ 33.3 ± 0.66	-1.2 ± 0.11 ~ 2.9 ± 0.44
TEF	8.4 ± 0.11 ~ 33.3 ± 2.07	-0.8 ± 0.12 ~ 4.9 ± 1.44

821 SAV, savanna woodland; TRF, tropical rain forest; STF, subtropical evergreen broad-
 822 leaved forest; TEF, temperate mixed forest.

823